V International Conference on Computational Methods for Coupled Problems in Science and Engineering
COUPLED PROBLEMS 2013
S. Idelsohn, M. Papadrakakis and B. Schrefler (Eds)

A COMPARATIVE STUDY OF COMPUTER MODELS FOR FRICTION AND THEIR INFLUENCE ON DYNAMICS OF THE HEAVY RIGID BODY ON A HORIZONTAL SURFACE

IVAN I. KOSENKO*

*Department of Technological Support of an Aircraft Reliability
Tsiolkovsky Russian State University of Technology
Orshanskaya st. 3, Moscow, 121552, Russia
e-mail: kosenko@ccas.ru, web page: http://www.mati.ru/

Key words: object-oriented modeling, multibond graph, canonical junction structure, rattleback, friction model, tippe-top

Abstract. Using an example of a heavy rigid body moving on a horizontal surface and having with it a permanent contact the process of construction and verification for spatial dynamical models of the multibody systems is analyzed. Two approaches to formal representation of the models: object-oriented, and bond graph based are applied. Energy based similarities between these approaches are analyzed.

A detailed description of the bond graph representation for the most general type of constraint is presented. It turned out the resulting total bond graph model of the multibody system dynamics always has exactly a so-called canonical junction structure. This representation has a tight correspondence with our object-oriented implementation of the mechanical constraint architecture. As an example Modelica implementation of several classes in the row for mechanical contact is investigated.

Computer implementations for three examples of the heavy rigid body dynamics are under investigation: (a) the rattleback, (b) example of A. P. Markeev, (c) the Tippe-Top. Among all of three examples each one demonstrates in its own manner a peculiar dynamical behaviour.

1 INTRODUCTION

Development of a computer model for multibody system (MBS) dynamics is a process needing in a reliable unified technology to construct the models in an efficient way. It turns out Modelica language provides a tools to resolve such a problem successively step by step using its natural approaches. One of them is connected tightly with the so-called multiport representation of the models initially based on the bond graph use. These latter based in turn on the idea of energy interaction, and substantially on energy conservation for physically interconnected subsystems of any engineering type.

Verification process is critically important for the reliable MBS dynamical model design. One has to remark that mechanical examples with friction are exclusively useful for testing process while verifying the model. In this way we apply several cases of MBS with contacts having well-known dynamical behavior to verify our library of classes for composing the MBS dynamical models.

2 BOND GRAPHS AS A BACKGROUND

Geometric formalisms to represent the multibody system (MBS) dynamics are well known [1]. These formalisms operate with known mechanical objects, twists and wrenches, having known information description concerning a causality in the MBS models. The model representation under consideration is tightly connected with the power based approach to modeling, so-called bond graphs [2].

Indeed, let the rigid body kinematics be defined by the twist $(\mathbf{v}, \boldsymbol{\omega})$, where $\mathbf{v}$ is the mass center velocity, and $\boldsymbol{\omega}$ is the body angular velocity. All velocities for definiteness assumed to be defined with respect to (w. r. t.) any base body rigidly connected with an inertial frame of reference. Further let all the forces acting upon the body be reduced to the wrench $(\mathbf{F}, \mathbf{M})$ with the total force $\mathbf{F}$ acting at the mass center and the total torque $\mathbf{M}$. Thus the total power of all the forces acting on the body is computed by the known formula

$$W = (\mathbf{v}, \mathbf{F}) + (\boldsymbol{\omega}, \mathbf{M})$$

being used for representing a multibond in the bond graph simulating the MBS dynamics. We have in such the case an evident canonical duality between twists and wrenches.

In our approach which is more natural in traditional classical mechanics we assume twist for the flow and wrench for the effort variable in the multibond. In the further course we present an illustration for this approach and demonstrate its convenience to construct the mechanical constraints of contact type in a relatively simple way. One can find also a description of other cases of constraints in [3].

Doing so we can associate dynamical object of the rigid body with 1-junction. The reason is that 1-junction has zero sum of efforts for all incident multibonds. We can simulate the d'Alembert principle using this latter property of the junction in the following way: one multibond connects this junction with its only element of inertance, while other multibonds deliver forces of different nature to the junction. Similarly, one can associate 0-junction with the (dynamical) object of mechanical interaction, constraint in particular. This time incident multibonds have zero sum of velocities (flow variables). 0-junctions of this type always have three multibonds each. Then one of incident multibond has a flow variable being a subtraction of two other multibond flows. This property exactly is one of relative velocity at contact.

Finally one can represent a general bond graph structure of the constraint in any MBS in a way as it is depicted in Figure 1. Triangles in the Figure: A, B correspond to interacting bodies, C denotes constraint or contact force element.

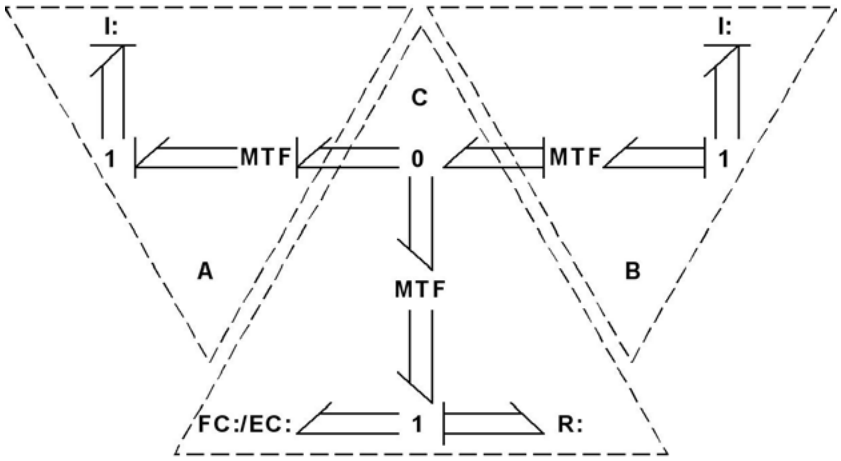

Figure 1: Bond graph representation of a constraint of general type

All multibonds here consist of the twist $(\mathbf{v}, \boldsymbol{\omega})$ signals representing the flow component, and the wrench $(\mathbf{F}, \mathbf{M})$ signals as an effort. Causality of an inertance elements arranges according to the Newton–Euler system of ODEs. Left and right transformers are to shift the twist from the mass center to the contact point P (being computed inside block C) according to the known Euler formula: $(\mathbf{v}, \boldsymbol{\omega}) \mapsto (\mathbf{v} + [\boldsymbol{\omega}, \mathbf{r}], \boldsymbol{\omega})$, where the vector $\mathbf{r}$ begins at the corresponding center of mass and ends at the contact point. Reciprocally the wrenches shift to the body mass center from point of the contact in a following way: $(\mathbf{F}, \mathbf{M}) \mapsto (\mathbf{F}, \mathbf{M} + [\mathbf{r}, \mathbf{F}])$. As one can see easily the transformers conserve the power. Central transformer is responsible for the transfer to orthonormal base at the contact point with the common normal unit vector and two others being tangent ones to both contacting bodies' surfaces supposed regular enough.

Note that it is a usual practice to attach the inertance element to 1-junction, in particular because of its causality nature, see for example [4, 5]. Figure 1 can remind us in some degree a bond graph element of the lumped model for the flexible beam dynamics.

Causality for some multibonds inside the constraint object is defined individually for each particular scalar bond [6] depending on the type of the constraint and is assigned finally after the whole MBS model compilation. If we will continue to build the bond graph model for the whole MBS in a proposed way then finally we can arrive exactly at the so-called canonical junction structure [6] useful for the formal procedures of the bond graph optimal causality assignment. For this we have to add an intermediate 0-junctions for elements attached to 1-junction in the constraint component C, see Figure 1.

Leaving some multibonds without the causality assignment and trusting this work to compiler we apply a so-called acausal modeling [7]. On the other hand if we will act in a manner close to the real cases of constraints with elasticity then instead of the constraint elements FC/EC, we have to use an element of the compliance with the causality uniquely determined

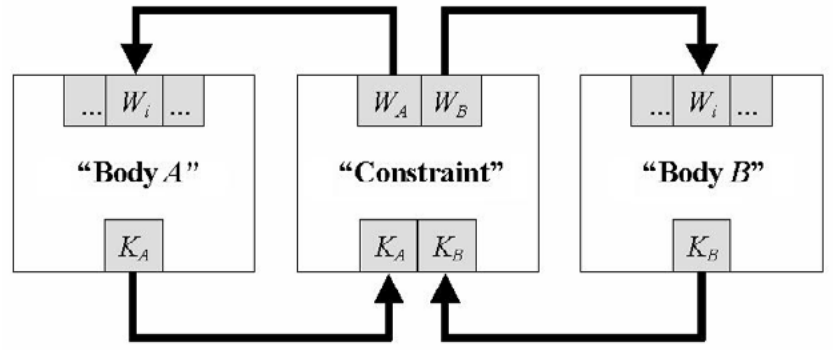

Figure 2: Architecture of constraint as a communication network

3 OBJECT–ORIENTED IMPLEMENTATION

When using Modelica language [8] we construct a unified computer model of the constraint, or, in a more general way, of any physical interaction between two rigid/deformable bodies we define [9, 10, 3] two classes of communication ports: (a) class of the kinematic port and (b) one of the effort port. These ones are twist and wrench connectors. It turned out the connections of such types make it possible to construct a model of the bodies interactions based on the causality physically motivated.

Briefly speaking we consider a constraint/contact between two rigid bodies as a communication network working in a following way. Namely, the constraint object imports the kinematic information, twists plus additional data, accepting it from the objects of interacting bodies and reciprocally exports wrenches (plus additional data) as a response in the opposite direction. Thus the constraint "computes" an efforts the bodies interact by, see Figure 2. And now we are going to point out the similarity between the bond graph description above and our MBS model. Indeed, the pair of twist/wrench ports plays a role of the multiport notion, and corresponding pairs of connections in Figure 2 stand for the notion of a bond with a causality identically defined.

Furthermore, in this way we can associate objects ob bodies with 1-junction each, while 0-junction is associated with the object of the constraint. A superclass of our package for objects of bodies encapsulates dynamics of rigid body and is described by means of Newton's differential equations for the body mass center, and by Euler's differential equations for the body rotation about it. The Euler equations are constructed using quaternion algebra [11].

If we use multiport concept for developing model of the MBS dynamics then the most complicated task is a design of the class hierarchy for the constraint/contact objects. A base constraint superclass is a root of such class hierarchy tree. According to Newton's third law this superclass must contain equations of the form

$$\mathbf{F}_A + \mathbf{F}_B = \mathbf{0}, \quad \mathbf{M}_A + \mathbf{M}_B = \mathbf{0}. \tag{1}$$

in its behavioral section. Here arrays $\mathbf{F}_A$, $\mathbf{M}_A$ and $\mathbf{F}_B$, $\mathbf{M}_B$ represent constraint forces

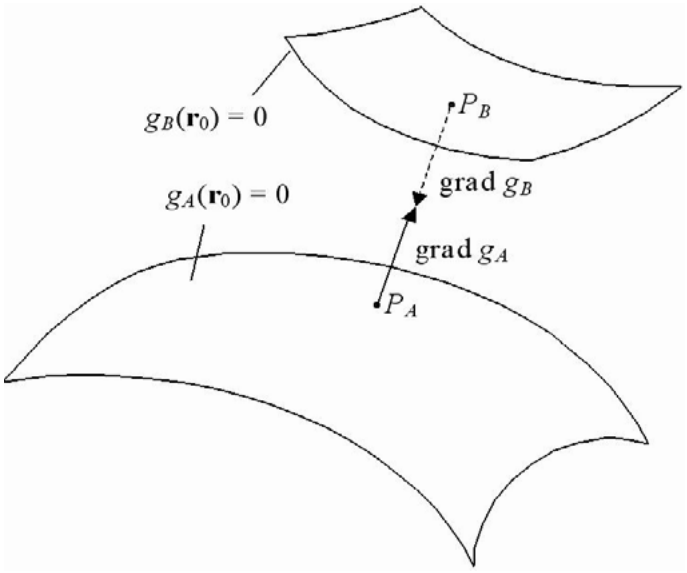

Figure 3: Area of contact vicinity

and torques "acting in directions" of bodies A and B respectively. Additional equations for different types of constraints are to be added to equations (1) in different classes–inheritors corresponding to these particular types of constraints. In order to derive these equations let us consider the local geometry of the problem, see Figure 3.

The base body of MBS supposed to be connected with the absolute frame $O_0x_0y_0z_0$ (AF) fixed in the inertial space (body A in our case is fixed platform with horizontal surface), $O_\alpha x_\alpha y_\alpha z_\alpha$ is the frame BF_α fixed in the body $\alpha \in \{A, B\}$. The outer surfaces Σ_α are defined by the equations $f_\alpha(\mathbf{r}_\alpha) = 0$ $(\alpha = A, B)$ w. r. t. appropriate BF_α whose axes are coincident to the principal central axes of inertia. In AF these the equations read $g_\alpha(\mathbf{r}_0) = f_\alpha[T^*_\alpha(\mathbf{r}_0 - \mathbf{r}_{O_\alpha})] = 0$ $(\alpha = A, B)$. Here $\mathbf{r}_{O_A} = O_0O_A$, $\mathbf{r}_{O_B} = O_0O_B$, T_A, T_B are the orthogonal matrices determining orientation of the BF_A and BF_B w. r. t. the AF. An asterisk denotes the matrix transposition. The functions $g_A(\mathbf{r}_0)$, $g_B(\mathbf{r}_0)$ depend upon the time indirectly through the variables $\mathbf{r}_A$, $\mathbf{r}_B$, T_A, T_B.

The constraint object of our model has to compute at each current instant the points $P_A \in A$ and $P_B \in B$ implementing the minimal distance between the bodies. These points depend on relative orientation of the bodies. By virtue of above assumptions such points are to be evaluated in a unique way. Denote by $\mathbf{r}_{P_A}$, $\mathbf{r}_{P_B}$ the radii vectors of these points w. r. t. AF. The simple geometric reasons imply the following system of algebraic equations

$$\begin{array}{rclcrcl} \operatorname{grad} g_A(\mathbf{r}_{P_A}) & = & \lambda \cdot \operatorname{grad} g_B(\mathbf{r}_{P_B}), & & g_A(\mathbf{r}_{P_A}) & = & 0, \\ \mathbf{r}_{P_A} - \mathbf{r}_{P_B} & = & \mu \cdot \operatorname{grad} g_B(\mathbf{r}_{P_B}), & & g_B(\mathbf{r}_{P_B}) & = & 0. \end{array} \tag{2}$$

The system (2) consists of eight scalar equations w. r. t. eight scalar variables: x_{P_A}, y_{P_A}, z_{P_A}, x_{P_B}, y_{P_B}, z_{P_B}, λ, μ, where λ, μ are auxiliary variables. The equations (2) are in

use either without or with a presence of the contact of bodies A, B. In the latter case the condition $\mu \leq 0$ satisfies. If we want to simulate the point contact case then the equation $\mu = 0$ is to be added to the model. According to computational experience it is more reliable and convenient to use the equations of constraints (2) in a differential form. When using this latter, i. e. differential, form of a constraint one needs to set a consistent initial values for the variables $\mathbf{r}_{P_A}$, $\mathbf{r}_{P_B}$, λ, μ at the start time instant of simulation. Further we analyze several dynamical examples of mechanical contact.

4 POINT-CONTACT CASE

Point contact is a simplest case under verification. As it was already mentioned to satisfy the point contact between the bodies we should satisfy the condition $\mu = 0$ for equations (2). For simplicity and definiteness from now on we assume satisfied the contact condition for the point-contact case and for the patch-contact one as well.

After that two possibilities remain: (a) relative sliding of bodies A and B outer surfaces at contact; (b) relative rolling at the contact point. Consider them successively decreasing number of degrees of freedom (DOFs) for relative motion at contact. Denote by $\mathbf{F}_A$ the force acting on the body A from the body B. And by $\mathbf{F}_B$ denote the force acting on the body B from one of A vice-versa. Each force cited acts at the point P_α, $\alpha = A, B$. In case of contact $P_A = P_B$. In addition, let us introduce auxiliary notations $F_{An} = (\mathbf{F}_A, \mathbf{n}_A)$, $\mathbf{F}_{A\tau} = \mathbf{F}_A - F_{An}\mathbf{n}_A$, $\mathbf{v}_r = \mathbf{v}_{P_A} - \mathbf{v}_{P_B}$, $v_{rn} = (\mathbf{v}_r, \mathbf{n}_A)$, $\mathbf{v}_{r\tau} = \mathbf{v}_r - v_{rn}\mathbf{n}_A$ where $\mathbf{n}_A$ is the outer normal to the body A surface at point P_A.

In case of bodies contact the condition $\mu = 0$ from above is equivalent to the kinematic one $v_{rn} = 0$. Cases of sliding and rolling differ one from another using conditions in a tangent plane. Implementation of the Coulomb friction model is assumed for the simplicity. Then one can obtain the vector force equation in the tangent plane

$$\mathbf{F}_{A\tau} - d \cdot F_{An} \frac{\mathbf{v}_{r\tau}}{|\mathbf{v}_{r\tau}|} - \kappa \mathbf{n}_A = \mathbf{0}, \tag{3}$$

where d is the coefficient of friction. Thus these latter three equations plus equation $v_{rn} = 0$ all combine the system of four scalar equations w. r. t. four scalars F_{Ax}, F_{Ay}, F_{Az}, κ.

When rolling the tangent velocity has to be zero $\mathbf{v}_{r\tau} - \kappa \mathbf{n}_A = \mathbf{0}$, and with equation $v_{rn} = 0$ we have four scalar equations once more for the same four variables of the MBS model.

Model equation (3) "works" properly in case of sliding if relative velocity is not very small. However the problem of regularization for the equation of constraint (3) arises when transposing from the state of rolling to one of sliding. It was found that one can apply here the known approximation for Coulomb's friction using regularized expression for the tangent force

$$\mathbf{F}_{A\tau} - \kappa \mathbf{n}_A = \begin{cases} d \cdot F_{An} \mathbf{v}_{r\tau} / |\mathbf{v}_{r\tau}| & \text{as} \quad |\mathbf{v}_{r\tau}| > \delta, \\ d \cdot F_{An} \mathbf{v}_{r\tau} / \delta & \text{as} \quad |\mathbf{v}_{r\tau}| \leq \delta, \end{cases}$$

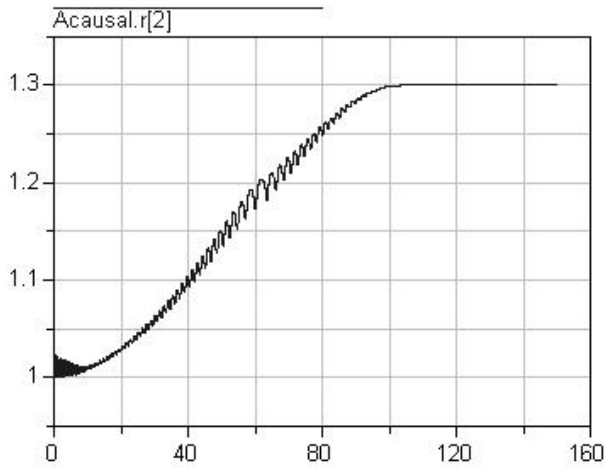

Figure 4: Center of mass altitude

where one supposes that $\delta \ll 1$.

It is known [12] that in this case the solution of the regularized problem remains close to the solution of the original one on asymptotically large time intervals. Implementation and further simulation show this closeness holds with the very high degree of accuracy. Such an approach resolves completely the problem of modeling for accurate transitions between states of sliding and rolling.

4.1 Example of A. P. Markeev

Consider the translational-rotational motion of the homogeneous rigid body of an ellipsoidal shape on the rough horizontal surface [13]. Friction assumed of the Coulomb type and regularized as above with the small coefficient $d = 0.01$. The body is set at initial instant on its smallest semi–diameter endpoint and spinned fast enough. For this case one can repeat easily an experiment described qualitatively by A. P. Markeev: the body in finite time "stands" on its largest semi–diameter.

In case of our example body's semi–diameters are close enough one to another: $a_1 = 1.2$, $b_1 = 1$, $c_1 = 1.3$. Axes of the body ellipsoidal surface coincide with ones of the central principal ellipsoid. Choosing initial data as follows: $\mathbf{r}(0) = (0, 1, 0)^T$, $\mathbf{v}(0) = (0.05, 0, 0)^T$, $\mathbf{q}(0) = (1, 0, 0, 0)$, $\boldsymbol{\omega}(0) = (0, -10, 2)^T$, one obtains the result cited above: the ellipsoid mass center "rises" progressively from the height of minimal semi–diameter to one of maximal semi–diameter, see Figure 4.

4.2 Example of the rattleback

Further consider dynamics of the rattleback playing a role of body B on an immovable horizontal surface [14] playing a role of body A. Usually the rattleback, or wobblestone, or celtic stone, is assumed being rigid body bounded by paraboloidal or ellipsoidal surface.

Central principal axes of inertia are rotated w. r. t. the body outer shape axes of symmetry. We consider the case of an ellipsoidal surface.

The model described above has been developed using Modelica package of classes for 3D dynamics of MBS. The high quality of an approximation for the rattleback motions has been verified through different simulations performed. In particular, computations corresponding to case of Kane and Levinson [14] have been performed. Results of simulations are identical in all slightest details.

5 PATCH-CONTACT CASE

The point contact model unable often to explain dynamic effects while elastic bodies contacting. If we introduce the patch as a result of elastic interaction then we have to construct proper model of compliance at contact. There is a lot of models of such nature. The Hertz contact model [15] is one of the most popular one among engineers. This model provides a reliable procedure of normal elastic force computation for interaction of two rigid bodies.

Local geometric reduction in vicinity of contact is similar to above one. The only difference is absence of the point case constraint $\mu = 0$. For the patch case the condition $\mu \leq 0$ should take place permanently. In the current case we suppose the bodies A and B don't create any obstacles for their relative motion. If 3D-regions bounded by the bodies outer surfaces do not intersect then the object of a contact, generates a zero wrench in the direction of each body. Simultaneously this object has to generate the radius vectors $\mathbf{r}_{P_A}$, $\mathbf{r}_{P_B}$ of opposing with each other points P_A, P_B, see Figure 3. One can find in [16] full detailed reduction and computational implementation of the Hertz model and its volumetric modification proposed by V. G. Vil'ke.

Elliptic patch arising in the Hertz model causes new effects in tangent friction forces behavior. The simplest friction model on this way is one of Contensou – Erismann [17, 18]. One can find in [19] details of this model computer implementation. One of the model key features is application of piece-wise continuous approximation for the wrench of friction forces distributed over the elliptic contact patch. Due to simplicity this approximation is efficient and has an implementation fast enough. Besides, verification of the model using the Tippe-Top example shows its satisfactory accuracy.

Unlike to previous considerations we construct here a so-called unrestricted contact problem. This latter means that we do not apply any preliminary assumptions about contact patch and normal force, what is usual in engineering practice. Instead we compute dynamically the patch and the normal force using the Hertz model (or its volumetric modification), and simultaneously we compute the total wrench of friction forces taking into account dimensions of contacting area permanently in time.

5.1 Example of the Tippe-Top

The general contact model including the Hertz model for normal forces and the Contensou–Erismann one for tangent forces has been verified here by two stages: (a) for the case of circular contact; (b) for the case of elliptic non-circular contact. The known Tippe-Top dynamical model was investigated as an example of the first case. All the parameters and initial conditions are exactly the same as in the paper [20] whose authors got these data in turn from the work [21].

The Tippe-Top body, supposed geometrically rigid, composed by two balls one of larger radius $R = 1.5 \cdot 10^{-2}$m, and another, smaller, one of the radius $r = 0.5 \cdot 10^{-2}$m. The top center of mass supposed resting at initial instant of motion. Besides the top itself, more accurately its larger ball, assumed without any initial penetration with the horizontal surface. The smaller ball is located on the upper hemisphere of the larger ball, and initially the top axis of symmetry bends w. r. t. vertical by the angle $\theta_0 = 0.1$rad. Initial angular velocity $\omega_0 = 180\text{s}^{-1}$ is directed along axis of the top symmetry.

In the model under development here we consider an unrestricted contact problem that is the normal force is computed from the Hertz (or V. G. Vil'ke) model with addition of some nonlinear viscous term. Simultaneously the contact area is computed too. Then all the data obtained are used to calculate the tangent force and the turning friction torque in frame of the simplified Contensou model.

Remarkably, a computational experiment showed the top revolution from "feet", the larger ball in contact, to "head", the smaller ball in contact, scenario well known in mechanics. Simultaneously, using the results of the paper [22] a verification procedure has been performed. Namely, exact formulae obtained by V. F. Zhuravlev in [22] for the friction force and for the turning friction torque, case (a), were applied to the top dynamics computer model implemented on Modelica language in frame of the unrestricted, in sense mentioned above, contact model. In the same dynamical frame the simplified Contensou model, case (b), as well as a linear-fractional Pade approximation for the friction force and torque, case (c), were also implemented. The results of the inclination angle evolution showed that revolution scenarios are mutually closest in cases (a) and (b). If we use the Pade approximations of higher order [24], then the resulting accuracy is improved. Results obtained in [20] were also completely verified.

Note in addition, one can easily obtain a behavior typical to the Tippe-Top, revolution to "head", in frame of the "regularized" Amontons–Coulomb friction. One has to understand regularization in a sense proposed in the works [12, 23] and used above in case of the point contact. We only have to "bend" graph for the friction force dependence on the relative slip velocity in vicinity of zero replacing its discontinuity by the linear function. The more flat slope of the graph the sooner one can find out the Tippe-Top revolution effect. As the simplified Contensou model shows that just this slope appears in the corresponding graph for the friction force dependence on the velocity, this time in frame of the exact Contensou–Erismann model.

5.2 Example of the ball bearing

The dynamical model of the ball bearing was considered in a way similar to the paper [19] while the verification of second stage. This time the contact area is essentially elliptic one. The main goal for the numeric simulations was to compare two approaches: (a) the standard Hertz model for the normal force plus the Contensou simplified model for the friction forces; (b) the simplified model of V. G. Vil'ke for the normal elastic force plus the Contensou simplified model for the friction forces. As it was observed in [19] for the case of the regularized Coulomb friction force here dynamical models of the cases (a) and (b) differ one from another in a slightest degree too. Simultaneously, the model (b) is faster than (a) by 20% meaning the CPU time needed.

6 CONCLUSIONS

Brief summary of some results obtained in the paper could include the following issues:

(a) unified multibond graph representation of the MBS dynamics in a sufficiently simple way with the canonical junction structure is possible.

(b) The representation depicted in Figure 1 can be used as a guideline for constructing the consistent system of DAEs in a systematic way. In other words we can say that multibond graph constructs like ones of Figure 1 are to be used as a regular basis for more informal object-oriented approach.

(c) An object-oriented representation makes it possible to develop the constraints models adopted to the specific types of the bodies interconnections in a fast and effective manner implementing the corresponding bond graph formalisms in a more natural and informal way mainly by chains of inheritance for the behavior (equations) and properties thus gradually filling the complete multibond graph description.

(d) An acausal modeling accelerates the modeling releasing a developer from the problem of causality assignment if s/he takes into account some requirements like complementarity rules.

(e) It turned out an introduction of the component of the ODEs system for the elastic bodies outer surfaces tracking for the contact problem conserves an accuracy and simultaneously improves the reliability of the models. To implement the tracking in case of the complex shape surfaces we have to rearrange only one derived class at the end of the inheritance chain to define an equations for the gradients and Hessians of the surfaces A and B w. r. t. LFs of the bodies.

(f) The algorithm of V. G. Vilke is more reliable and suitable for wide range of the contact area eccentricities simultaneously providing an accuracy of 0.5% with respect to the Hertz-point algorithm.

(g) The Tippe-Top "on head" revolution effect is caused completely by the dry friction force "regularization" in vicinity of zero value for the velocity of relative slip. Such a regularization takes place exactly in the Contensou–Erismann model. Numeric experiments showed if the slope of friction force graph in vicinity of the zero velocity in the regularized

Coulomb model is steep enough then the Tippe-Top effect either isn't observed at all or arising during short time after a long evolution then vanishes quickly. And only noticeable decreasing of the slope mentioned immediately causes the top revolution on the "head" with the subsequent long precession in this position.

7 ACKNOWLEDGEMENTS

This work was performed with partial support of Russian Foundation for Basic Research, projects: 11-01-00354-a, 12-01-00536-a, 12-08-00637-a.

REFERENCES

[1] Stramigioli, S., Blankenstein, G., Duindam, V., Bruyninckx, H., Melchiorri C. *Power port concepts in robotics. The Geometrical–Physical Approach*. Tutorial at 2003 IEEE International Conference on Robotics and Automation. IEEE, (2003).

[2] Paynter, H. M. *Analysis and design of engineering systems*. The M. I. T. Press, (1961).

[3] Kosenko, I. I. Physically oriented approach to construct multibody system dynamics models using Modelica language. *Proceedings of Multibody 2007, Multibody Dynamics 2007*. An ECCOMAS Thematic Conference, Politecnico di Milano, Milano, Italy, (2007).

[4] Cellier, F. E. *Continuous System Modeling*. Springer–Verlag, (1991).

[5] Mukherjee, A., Karmakar, R. *Modelling and Simulation of Engineering Systems through Bondgraphs*. Alpha Science International Ltd., (2000).

[6] Golo, G. *Interconnection Structures in Port-Based Modelling: Tools for Analysis and Simulation*. PhD Thesis. University of Twente, Enschede, The Netherlands, (2002).

[7] *Dymola. Dynamic Modeling Laboratory. User Manual. Volume 1. Dymola 7.3*. Dynasim AB, Research Park Ideon, Lund, (2009).

[8] Fritzson, P. *Principles of object-oriented modeling and simulation with Modelica 2.1*. IEEE Press, (2004).

[9] Kossenko, I. I. and Stavrovskaia, M. S. How one can simulate dynamics of rolling bodies via Dymola: approach to model multibody system dynamics using Modelica. *Proceedings of the 3rd International Modelica Conference*, Linkopings universitet, Linkoping, Sweden, (2003) 299–309.

[10] Kossenko, I. I. Implementation of unilateral multibody dynamics on Modelica. *Proceedings of the 4th International Modelica Conference*, Hamburg University of Technology, Hamburg–Harburg, Germany, (2005) 13–23.

[11] Kosenko, I. I. Integration of the equations of the rotational motion of a rigid body in the quaternion algebra. The Euler case. *Journal of Applied Mathematics and Mechanics*, (1998) **62**:193–200.

[12] Novozhilov, I. V. *Fractional analysis : methods of motion decomposition*. Birkhauser, (1997).

[13] Markeev, A. P. On the motion of an ellipsoid on a rough surface with slippage. *Journal of Applied Mathematics and Mechanics*, (1983) **47**:260–268.

[14] Kane, T. R. and Levinson, D. A. Realistic mathematical modeling of the rattleback. *International Journal of Non–Linear Mechanics*, (1982) **17**:175–186.

[15] Hertz H. Über die Berührung fester elastischer Körper. *J. reine und angewandte Mathematik*, (1882) **92**:156–171.

[16] Vil'ke, V. G., Kosenko, I. I., Aleksandrov, E. B. On computer implementation of the Hertz elastic contact model and its simplifications. *Regular and Chaotic Dynamics*, (2009) **14**:693–714.

[17] Contensou, P. Couplage entre frottement de glissement et frottement de pivotement dans la théorie de la toupie. *Kreiselprobleme Gyrodynamics: IUTAM Symposium Celerina*, 1962, Springer, (1963) 201–216.

[18] Erismann, Th. Theorie und Anwendungen des echten Kugelgetriebes. *Z. angew. Math. Phys.*, (1954) **5**:355–388.

[19] Kosenko, I. I., Aleksandrov, E. B. Implementation of the Contensou–Erismann tangent forces model in the Hertz contact problem. *Multibody System Dynamics*, (2010) **24**:281–301.

[20] Leine, R. I. and Glocker, Ch. A set-valued force law for spatial Coulomb–Contensou friction. *Europian Journal of Mechanics A/Solids*, (2003) **22**:193–216.

[21] Friedl, C. *Der Stehaufkreisel. Master's thesis*. Institut für Physik, Universität Augsburg (1997).

[22] Zhuravlev, V. F. The model of dry friction in the problem of the rolling of rigid bodies. *J. Appl. Math. Mech.*, (1998) **62**:705–710.

[23] Rooney, G. T. and Deravi, P. Coulomb friction in mechanism sliding joints. *Mechanism and Machine Theory*, (1982) **17**:207–211.

[24] Kireenkov, A. A.. Coupled model of sliding and spinning friction. *Doklady Physics*, (2011) **56**:626–631.